Available online at www.sciencedirect.com
SCIENCE DIRECT
Polymer 46 (2005) 2452–2460
polymer
www.elsevier.com/locate/polymer

Photophysical study of a conjugated–non-conjugated PPV-type electroluminescent copolymer

A.M. Machado[a,b], J.D. Da Motta Neto[a], R.F. Cossiello[c], T.D.Z. Atvars[c], L. Ding[d], F.E. Karasz[d], L. Akcelrud[a,*]

[a]*Departamento de Química, Universidade Federal do Paraná, Centro Politécnico, Caixa Postal 19081, 81531-990 Curitiba/PR, Brazil*
[b]*Instituto Tecnológico para o Desenvolvimento LACTEC, Centro Politécnico, 81531-990 Curitiba/PR, Brazil*
[c]*Instituto de Química, Universidade Estadual de Campinas, Caixa Postal 6154, 13084-971 Campinas/SP, Brazil*
[d]*Department of Polymer Science and Engineering, University of Massachusetts, Amherst, MA 01003, USA*

Received 4 November 2004; accepted 4 February 2005

Abstract

This paper reports the photo- and electroluminescence studies of emitting species of one of the first reported blue emitters, the conjugated–non-conjugated multi-block copolymer, poly[1,8-octanedioxy-2,6-dimethoxy-1,4-phenylene-1,2-ethenylene-1,4-phenylene-1,2-ethenylene-3,5-dimethoxy-1,4-phenylene]. Because the conjugation length of the emissive center is very well defined (two and half phenylene–vinylene units) the differences found between the fluorescence profile of the fluorophore in solution, at several concentrations and that in the solid state allowed us to conclude that in solid the emission comes from associated forms, such as ground-state dimers and/or excimers. Time-resolved fluorescence in a nanosecond time scale recorded at $\varpi_{em} = 24{,}096\ cm^{-1}$ showed a monoexponential decay of 1.5 ns, which is compatible with rigid forms of stilbene derivatives.

Keywords: Electroluminescence; Photoluminescence; Conjugated–non-conjugated block copolymer

1. Introduction

Studies on copolymers in which a well-defined emitting unit is intercalated with non-emitting blocks have demonstrated that the emitted color is not affected by the interspacer non-conjugated length. Nevertheless, the EL efficiency of the single layer LEDs fabricated with this type of copolymer depends on the length of the non-conjugated blocks: copolymers where longer spacers yielded higher-efficiency devices [1–5]. Those conjugated–non-conjugated copolymers are soluble, uniform in terms of conjugation length and can be designed to emit in any portion of the visible spectrum [6–9]. For example, it has been demonstrated that the device efficiency increases by up to 30 times in the prototypical polymer poly-(phenylene vinylene) (PPV) [10] with random interruption of conjugation by saturated groups in relation to the corresponding PPV devices [11].

One of the first reported conjugated–non-conjugated EL copolymers was the blue emitter containing PPV type blocks (2,1/2PPV units) interspersed among octamethylene sequences, that is, poly[1,8-octanedioxy-2,6-dimethoxy-1,4-phenylene-1,2-ethenylene-1,4-phenylene-1,2-ethenylene-3,5-dimethoxy-1,4-phenylene] [8], whose chemical structure is shown in Fig. 1. The EL properties of a device produced with this material are well documented, but, to our knowledge, the exact nature of the emitting centers has not been explored. In this study we describe some results obtained by dynamic fluorescence decays and steady-state fluorescence emission in an effort to identify the species responsible by the mechanism of photo- and electroluminescence processes.

* Corresponding author. Tel.: +55 413 367 507.
E-mail address: akcel@onda.com.br (L. Akcelrud).

0032-3861/$ - see front matter © 2005 Elsevier Ltd. All rights reserved.
doi:10.1016/j.polymer.2005.02.007

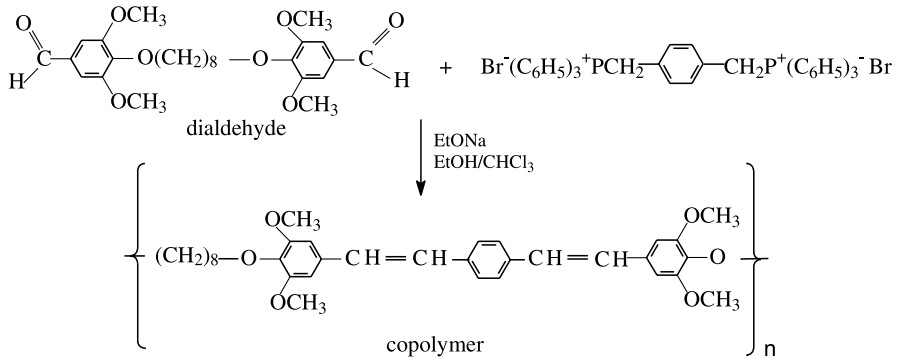

Fig. 1. Synthetic route and structures of dialdehyde and multi block conjugated–non-conjugated copolymer.

2. Experimental

2.1. Materials

Dimethylformamide (Vetec, Brazil) was distilled under vacuum (5 mm Hg) and stored under molecular sieves (4 Å). Ethanol was firstly refluxed with CaO (Vetec, Brazil) during 24 h and after distilled. 3,5-dimethoxy-4-hydroxybenzaldehyde (Aldrich), 1,9-dibromooctane (Aldrich), *p*-xylene-bis(triphenylphosphonium bromide) (Aldrich), metallic sodium, hydrochloric acid, iodine, sodium carbonate (Vetec, Brazil) were used without further purification.

2.2. Monomer synthesis and polymerization

The monomer synthesis was performed according to published procedures [2,8]. The polymer was prepared by classical Wittig condensation [2].

2.3. Methods

2.3.1. Molecular weight determination

A Waters gel permeation chromatograph equipped with two columns HR4E and HR5E (polystyrene), pump model 1500 was used. The solvent was DMF, in a flux of 0.6 ml min^{-1}, at 27 °C and the columns were connected to a dual detector (UV, refraction index), and the calibration was based on PS standards.

2.3.2. Absorption and fluorescence spectroscopies

A UV–Vis Shimadzu model NIR 3101 was used for the absorption measurements. Steady-state fluorescence spectroscopy was performed in a ISS-PC1 spectrofluorimeter operating with a 300 W Xe arc lamp, with excitation wavenumber ca. $\varpi_{exc}=27{,}027\ cm^{-1}$ (370 nm), collecting the emission from $\varpi_{em}=18{,}000–26{,}000\ cm^{-1}$ (560–400 nm). In addition, excitation spectra were also recorded from $\varpi_{exc}=33{,}333–20{,}000\ cm^{-1}$ (300–500 nm) with $\varpi_{em}=22{,}831\ cm^{-1}$ (438 nm). Emission and excitation spectra were performed with a triangular cuvette, as recommended when concentrated solutions are analyzed, to minimize the inner filter effect.

Dynamic fluorescence decay, at room temperature, was performed by single photon counting (Edinburgh Analytical nF900 system) operating with a pulsed hydrogen lamp at a repetition rate of 40 kHz. The excitation wavenumber was coincident with the excitation peak $\varpi_{exc}=27{,}027\ cm^{-1}$ for the chromophoric block absorption. The emission wavenumber for the collection of counts was in the fluorescence maximum $\varpi_{em}=24{,}096\ cm^{-1}$ (415 nm) for the chromophoric block. The sample solutions were degassed and maintained in a sealed quartz tube. The sample films were also degassed and sealed in a rectangular capilar. The instrument's response was determined at every measurement using Ludox® as scatterer. At least 10^4 counts were collected in the peak channel. Deconvolution of the lamp pulse was performed by nonlinear least-squares routines using the software supplied by Edinburg. The best fit was achieved when the χ^2 is close to one and the residual distribution is random.

2.3.3. FTIR and ^1H and ^{13}C NMR

The monomers and the polymer were characterized by FTIR and NMR and the data are compared with the literature. Samples for FTIR measurements were prepared as KBr disks. Spectra were taken in a Bomem MB 100 FTIR Spectrophotometer, in the spectral range of 600–4,000 cm^{-1}, with resolution of 2 cm^{-1}, and 16 scans.

A NMR Brücker 400 MHz Advance series with ^{13}C at 100 MHz and ^1H at 400 MHz equipment or an AC 200 MHz Brücker with ^{13}C at 50 MHz and ^1H at 200 MHz were used. All NMR experiments used $CDCl_3$ as a solvent and TMS as internal standard.

2.3.4. Device fabrication

Solutions of polymer (20 mg/ml in chloroform) were filtered through 0.2 μm Millex-FGS Filters (Millipore Co.) and were then spin coated onto PEDOT/Indium tin oxide (ITO)-coated glass substrates (OFC Co.) under nitrogen. Calcium layer (thickness ca. 400 nm) was evaporated onto the polymer at about 10^{-7} Torr, followed by a protective coating of aluminum. The devices were characterized using a system described elsewhere [12]. PL measurements were carried out using cast films onto quartz surfaces 'in situ'.

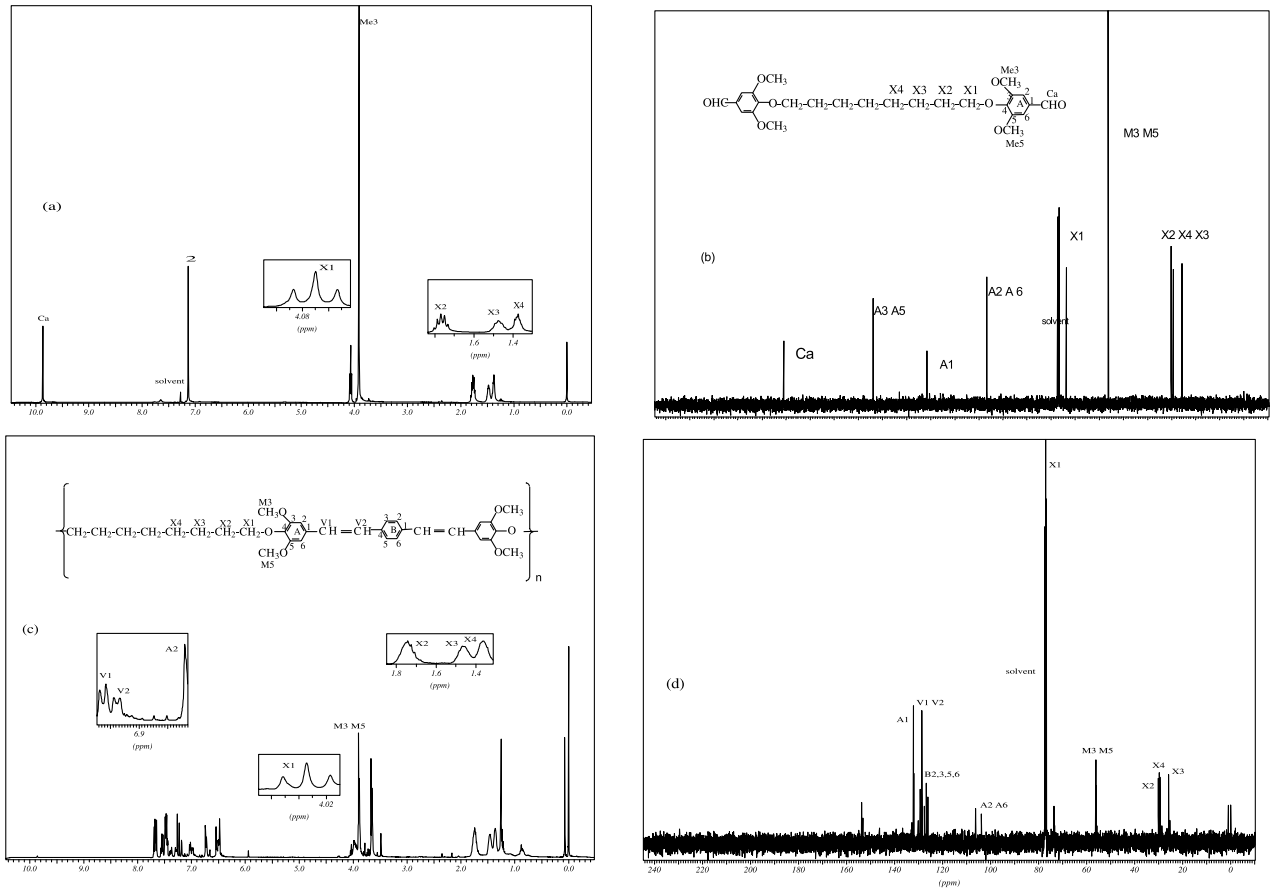

Fig. 2. ^{1}H NMR and ^{13}C NMR spectrum of dialdehyde and copolymer in $CDCl_3$ solution; (a) ^{1}H NMR of the dialdehyde; (b) ^{13}C NMR of the dialdehyde; (c) ^{1}H NMR of the copolymer; (d) ^{13}C NMR of the copolymer.

The thickness was adjusted in order to assure an optical behavior according to Beer's law.

2.3.5. Quantum chemical calculations

Quantum chemical calculations have been carried out for the monomer, dimer and trimer sequences. For each oligomer, geometries have been fully optimized, using the AM1 Hamiltonian of Dewar and coworkers [13,14]. In this step, we have used the MOPAC code. Due to the large number of atoms involved in the calculations, we have established a residual gradient norm of about 5.0 as a reasonable figure. Optimization was carried out in Cartesian coordinates (keyword *XYZ*), because optimization of internal coordinates proved too difficult to achieve. For each optimized structure, electronic absorption spectra have been simulated with the INDO/S technique as suggested by Zerner [15,16]: the reference determinant was obtained at the self-consistent field (SCF) level using the intermediate neglect of differential overlap (INDO/1) Hamiltonian, and the electronic spectrum was obtained by a subsequent configuration interaction (CI) calculation which included the reference determinant plus singly excitations only. The usual routine in INDO/S calculations defines the CI active space in terms of the energy separation between MOs near the Fermi level in the reference determinant. For instance, for the monomer one of the largest gaps in highest occupied molecular orbitals (HOMOs) is 0.023 Hartree between MO #101 and MO #102. One of the largest gaps in lowest unoccupied molecular orbitals (LUMOs) is 0.015 Hartree between MO #121 and MO #122. Therefore, the active space included all MOs between #102 and #121. We tried several variations in the size of the CI space, and the resulting spectrum did not change except for a couple of wavenumbers. That suggests that our results are consistent. All calculations have been carried out under FreeBSD operational system.

3. Results and discussion

3.1. Copolymer characterization

Molecular weight was determined as $\bar{M}_w = 41$ kg mol^{-1} and $\bar{M}_n = 29$ kg mol^{-1} with polydispersity index of ca. 1.44. The copolymer's structure was characterized by ^{1}H NMR and ^{13}C NMR spectra. Fig. 2 shows the assigned ^{1}H NMR and ^{13}C NMR spectra for the dialdehyde and copolymer.

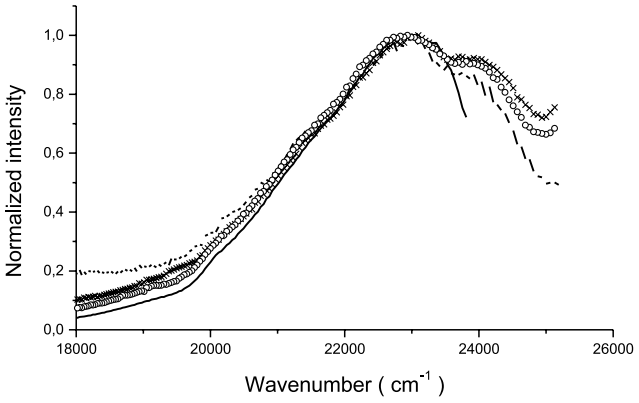

Fig. 3. Normalized fluorescence spectra of the copolymer in $CHCl_3$ solutions, $\varpi_{exc}=27{,}027\ cm^{-1}$ (370 nm). Concentrations: 10^{-6} mol l^{-1} (-x-x-), 10^{-5} mol l^{-1} (—), 10^{-4} mol l^{-1} (- - -), 10^{-3} mol l^{-1} (-o-o-).

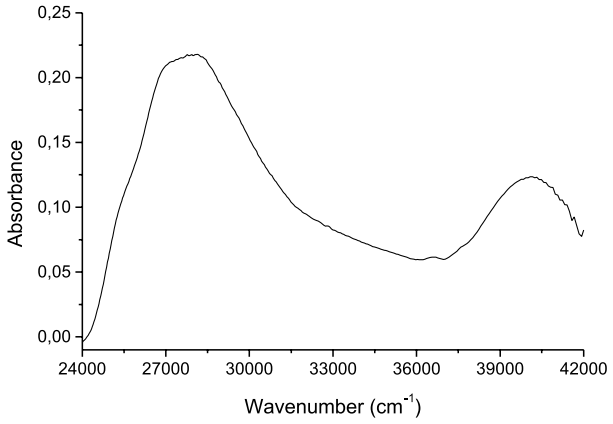

Fig. 5. Absorption spectrum of the copolymer in solution of $CHCl_3$. Concentration: 10^{-5} mol l^{-1}.

NMR and FTIR (not shown) results are consistent with those reported in the literature [6].

3.2. Emissive properties

Fig. 3 presents the fluorescence spectra ($\varpi_{exc}=27{,}027\ cm^{-1}$) of solutions of concentrations 10^{-3}–10^{-6} mol l^{-1}. Spectra of polymer solutions showed similar profiles being composed by a broad band peaking at $\varpi_{em}=23{,}094\ cm^{-1}$ (433 nm) resulting from the overlapping of vibronic bands, with a higher energy shoulder at $23{,}980\ cm^{-1}$ (417 nm). Increasing the concentration up to 10^{-3} mol l^{-1} reduced the relative intensity of the blue-edge of the emission band and the spectra became narrower. This observation can be explained by either the presence of the inner filter effect with reabsorption of the higher energy emission or by the formation of emitting aggregated species. As we have employed a triangular cuvette, we have assumed that although minimized, the inner effect could not be neglected. On the other hand, the presence of aggregates or associated polymer chains should increase the relative intensity of the red-edge, in addition to the decrease of the blue-edge, if there were fluorescent, which was not the case. This lead to the conclusion that in solution the aggregates exhibited a low fluorescence quantum yield or were not present at all.

The excitation spectrum for all solutions, with $\varpi_{em}=22{,}780\ cm^{-1}$ are shown in Fig. 4. The spectra of the diluted

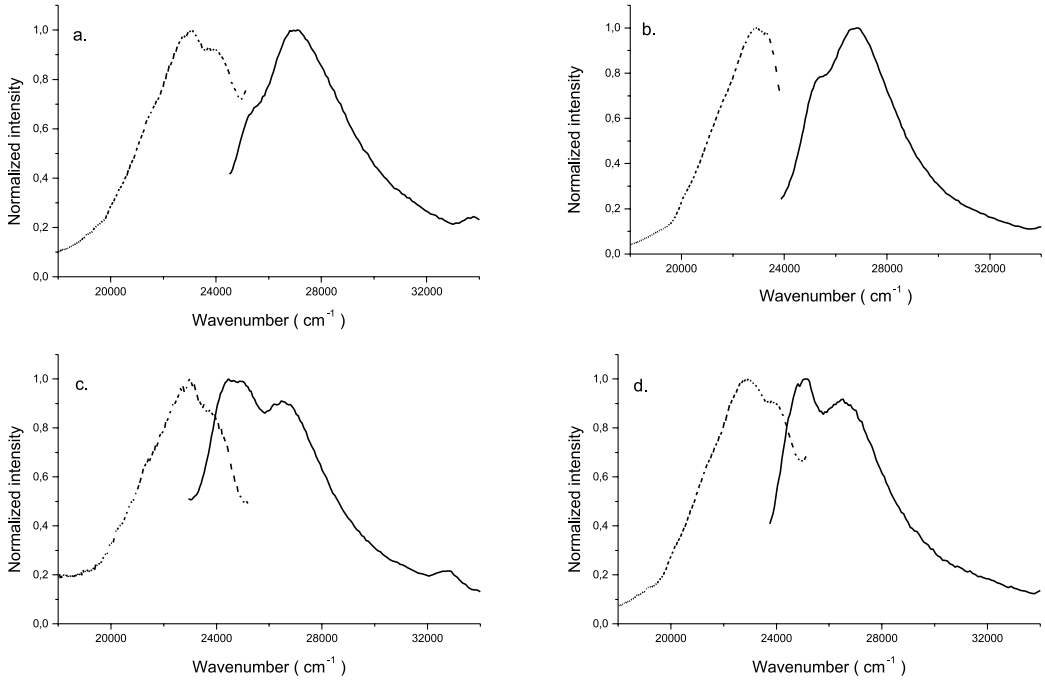

Fig. 4. Fluorescence ($\varpi_{exc}=27{,}027\ cm^{-1}$) (370 nm) (—) and excitation ($\varpi_{em}=22{,}780\ cm^{-1}$) (439 nm) (- - -) spectra of the copolymer in solutions of $CHCl_3$: (a) 10^{-6} mol l^{-1}, (b) 10^{-5} mol l^{-1}, (c) 10^{-4} mol l^{-1}, (d) 10^{-3} mol l^{-1}.

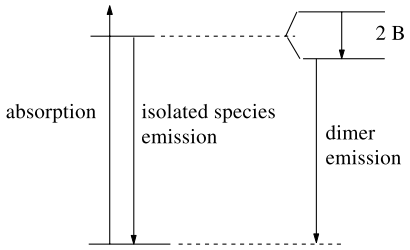

Fig. 6. Exciton splitting for a dimer compared to the isolated lumophore. 2 B is the Davidov splitting.

solutions 10^{-6} and 10^{-5} mol l^{-1} (Fig. 4(a) and (b)) were similar to the absorption spectrum (Fig. 5), the band is centered at $\varpi_{exc}=27{,}027\ cm^{-1}$ (370 nm) with a shoulder at $25{,}580\ cm^{-1}$ (390 nm) and were the mirror image of the emission spectrum at the same concentration, with a large Stokes shift ($\varpi_{exc}-\varpi_{em}\approx 3{,}933\ cm^{-1}$). This behavior is characteristic of the emission of an isolated chromophore, the conjugated segment corresponding to two and half phenylene vinylene units, in this case.

The excitation spectra of concentrated solutions (10^{-4} M and 10^{-3} mol l^{-1}, Fig. 4(c) and (d)), however, are split into two bands at$\varpi_{exc}=25{,}125$ and $26{,}525\ cm^{-1}$. Since the emission spectra were centered at $\varpi_{em}=22{,}935\ cm^{-1}$ (Fig. 3), a smaller Stokes shift ($\varpi_{exc}-\varpi_{em}\approx 3190\ cm^{-1}$) was obtained. Simultaneous changes of both excitation and emission spectra, recorded under conditions that minimize the inner effect, are usually attributed to the excitonic splitting observed when ground state dimers are formed [17]. Similar results have already been obtained with substituted stilbenes [18].

Assuming that the splitting of the excitation bands were originated from dimer by an excitonic effect, the Davidov splitting energy (2 B) [19] could be estimated from the difference between the excitation maximum of the isolated chain in diluted solution ($\varpi_{exc}=27{,}027\ cm^{-1}$) (Fig. 4(a)) and the excitation maximum of split peak in concentrated solution ($\varpi_{exc}=25{,}125\ cm^{-1}$) (Fig. 4(d)) as being ca. $1{,}902\ cm^{-1}$. For illustration, see scheme in Fig. 6. The red-shift of the excitation spectra suggests, according to the same exciton splitting model, that the relative orientation of

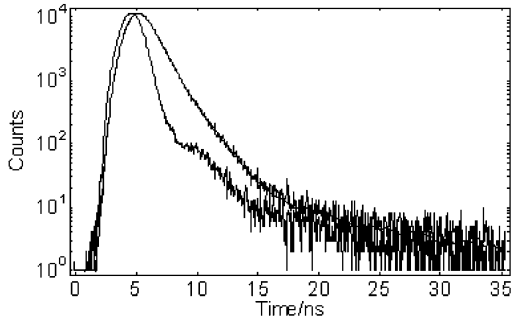

Fig. 7. Fluorescence decay of the copolymer (10^{-3} M in $CHCl_3$). $\varpi_{em}=22{,}883\ cm^{-1}$ (437 nm), $\varpi_{exc}=27{,}027\ cm^{-1}$ (370 nm). This includes: lamp profile and the superimposed best fit to the experimental data.

the two dipole moments of the molecules in the dimer is parallel and with opposite direction [19]. This exciton splitting in the range of 1,200–3,000 cm^{-1} is similar to that of small molecules and is compatible with an interplanar distance of 3–5 Å [19,20].

The photoluminescence quantum yield of the copolymer in diluted solutions (measured with 9,10-diphenylanthracene as standard) [17] was $\varphi_F=0.35$, substantially higher than that of *trans*-stilbene, $\varphi_F=0.07$ in the same solvent. This could be explained by the increase in the rigidity and planarity of the polymer-tied chromophore in relation to the 'free' stilbene. Longer lifetime of stilbene derivatives were attributed to the increase of their structural rigidity (i.e. more rigid forms have higher quantum yields and also longer lifetimes) [21].

The fluorescence lifetime for the copolymer measured in 10^{-3} M chloroform solutions, was 1.19–1.20 ns, (Fig. 7). Under the instrumental conditions employed here only decays longer than 0.5 ns could be recorded. Experimental curve profile can be fitted using a monoexponential function, with $\chi^2=0.991$ and good residual random distribution, but the existence of lifetimes faster than 0.5 ns cannot be excluded. Reported lifetimes for stilbene and stilbene derivatives have been extensively explored in the literature [21,22] but an unquestionable agreement is still needed. Lifetimes spanning from 0.14 to 1.8 ns, with mono and bi-exponential decays have been found [23,24]. Different emission mechanisms have been also proposed. In some cases monoexponential decay is suggested [21] whereas others defend a biexponential decay [25]. According to our data and with the higher value for the quantum yield for the copolymer in solution, the longer observed decay ca. 1.20 ns is explained by the larger rigidity of the polymer chain compared to the free lumophore. As the temporal resolution of our instrument does not cover the pico-second scale, excitation with other wavelengths was not done, since that will not add more information about the aggregation state of the emitting center.

The profile of the fluorescence band (PL) of the copolymer in the solid state, shown in Fig. 8, is red-shifted ($\varpi_{em}=22{,}124\ cm^{-1}$) in relation to the spectrum of the polymer in chloroform diluted (Fig. 4(a)) ($\varpi_{em}=23{,}094\ cm^{-1}$) and concentrated (Fig. 4(d)) solutions ($\varpi_{em}=22{,}935\ cm^{-1}$). Red-shift of the emission band of conjugated polymers in solid state compared with solutions can be attributed to several factors: increase of the critical conjugation length; energy transfer processes from shorter to longer chains; presence of associated interchain species in the electronic ground state (dimers) or in the electronic excited state (excimers) [26–32]. Considering that the conjugation length of this PPV-type copolymer is defined by its chemical structure and no further increase of the length can be imposed by the rigidity of the medium, the spectral red-shift must be attributed to the presence of associated interchain species (dimer or excimer). The vibronic structure of the PL spectrum evidenced by the

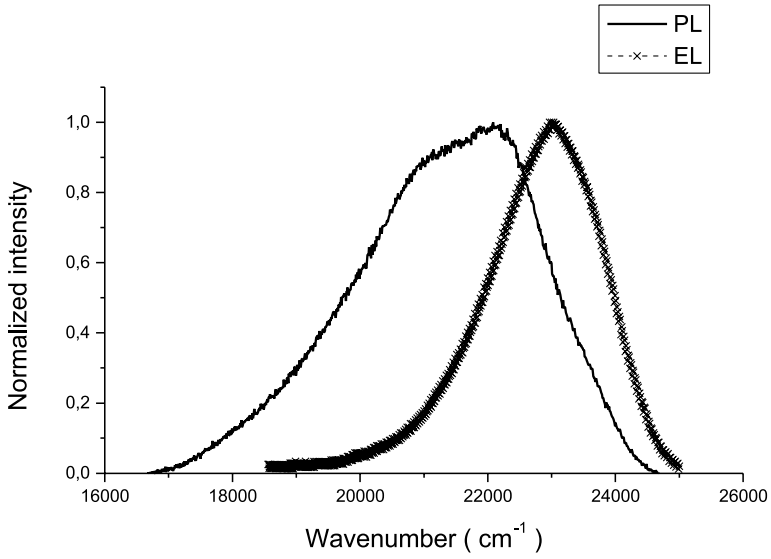

Fig. 8. Photoluminescence (—) and electroluminescence (-x-x-) spectra. EL device: (ITO/PEDOT/copolymer/Ca).

shoulder at 21,053 cm^{-1} suggests that the ground state dimer is the most probable associated species.

Differently, the electroluminescence spectrum is centered at $\varpi_{em}=21{,}186\ cm^{-1}$, coincident with the vibronic shoulder of the PL spectrum. Although we could explain the differences between the PL and the EL considering that the EL is usually generated near the Ca (opaque electrode) and to be detected should travel throughout the film thickness, increasing the probability of being partially self-absorbed, we consider that this possibility does not play an important role because we are working with very thin films. In addition, inner effect and radiative energy transfer processes should decrease the intensity at the blue-edge of the emission band, which has not been observed. We suggest that the red shift of the EL spectrum compared to the PL spectrum is related to the different emission zone in the thin films. The injected charge carriers may recombine and give rise to radiative emission in the area close to the polymer/Ca interface due to the unbalanced double injection possibly occurring in the devices. The tailing in the long wavelength region is largely due to defects in the emissive polymer layer which act as new recombination centers in which excitons radiatively decay giving emissions different from those from the pristine polymer backbone [33–35].

However, this is not the only reason for the differences between EL and PL spectra in the solid state. It is well known that the fundamental mechanisms generating the excitonic states in the EL (charge recombination) or PL (direct excitation) processes differ. The chain segments involved in these distinct processes may also differ. When an excitonic species is formed the environment surrounding these segments has to relax to stabilize the new dipolar orientation. If both recombination and emission processes are either faster or slower than the reorientation process then the EL and PL emanations from a relaxed Franck–Condon state are expected to be similar. However, if excitonic decay is faster, and recombination is slower than the average polymer relaxation time, these two emissions can be distinct as is the case observed here.

Taking into account the results presented so far (steady state fluorescence spectra, excitation spectra and fluorescence decays), we propose that the blue emitting species in either in PL or in electroluminescent devices of poly[1,8-octanedioxy-2,6-dimethoxy-1,4-phenylene-1,2-ethenylene-1,4-phenylene-1,2-ethenylene-3,5-dimethoxy-1,4-phenylene] are the ground state dimers and aggregates in the solid state. Since excimers cannot be directly excited, they cannot be observed by excitation spectroscopy and although their formation could not be detected, their occurrence evidently cannot be discarded.

We have already shown [18] that polar substituents bring about a strong tendency of aggregation in stilbene derivatives, red-shifting the emission [18]. As with other substituents, the four methoxy-groups in the aromatic rings of the conjugated segment of that polymer are probably acting in same direction, increasing the probability of aggregation. In addition, the inter-chain interaction and the creation of new excited state species has been the subject in recent proposals from the spectroscopic data, mainly related to PPV [12,36], and PPV derivatives, such as poly(2-methoxy-1,4 PPV) (MEH-PPV) [12,37] CN-PPV [38–40], poly(*p*-pyridyl vinylene) [41,42], acetoxy-PPV [43] and other light-emitting polymers [44–46] leading to evidences that interchain excitations play a significant role in the emission processes.

3.3. Quantum chemical calculations

Energies of the several molecular orbitals have been determined for the optimized geometry of the monomer,

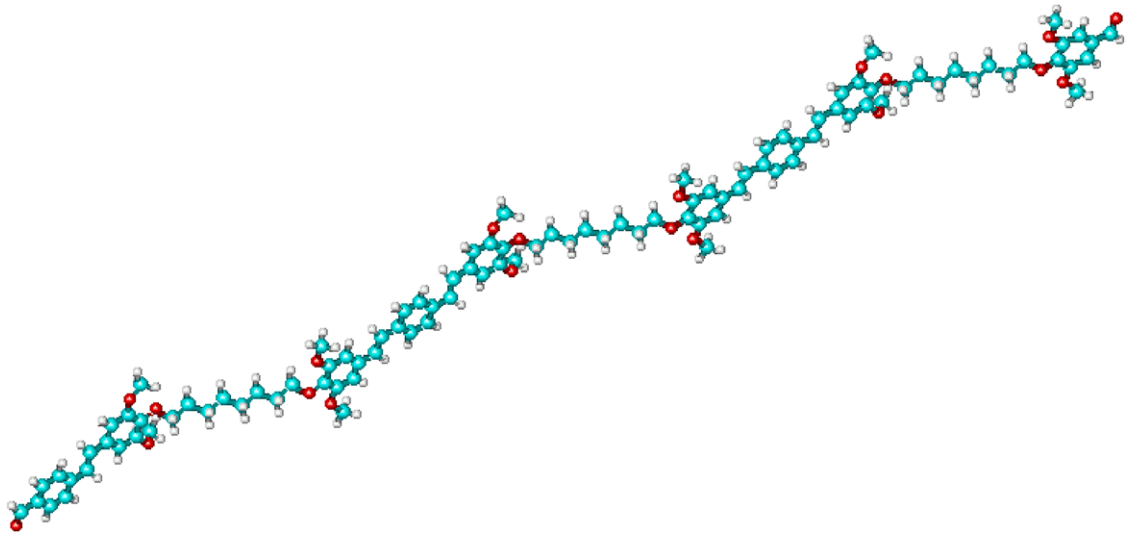

Fig. 9. Optimized AM1 geometry of the isolated trimer.

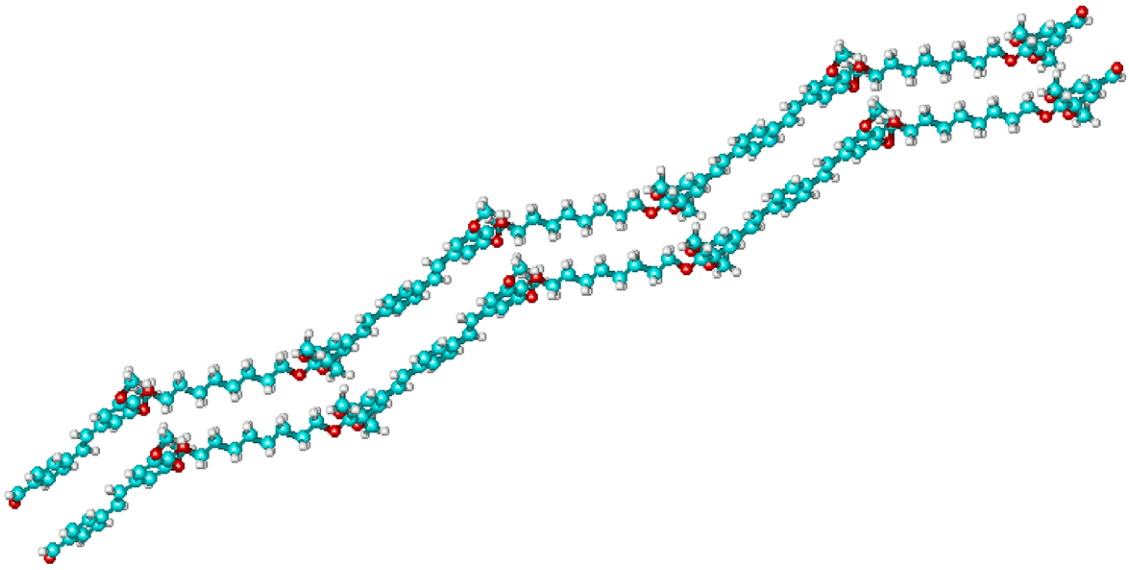

Fig. 10. Optimized AM1 geometry of the two associated trimers.

Table 1
INDO/S calculated absorption spectrum for the trimer, dimer and monomer of the isolated molecules

CI vector	Trimer		Dimer		Monomer	
	ν (cm^{-1})	$f_{osc.}$	ν (cm^{-1})	$f_{osc.}$	ν (cm^{-1})	$f_{osc.}$
2	28,742	2.5230	28,851	0.0003	28,433	0.0004
3	29,520	1.7080	31,746	0.5226	28,851	0.0003
4	33,242	1.2363	32,235	0.8890	31,746	0.5226
5	35,554	0.0072	32,618	0.0027	32,235	0.8890
6	36,047	0.0199	34,733	0.0005	32,618	0.0027
7	38,082	0.3333	37,791	0.2186	34,733	0.0005
8	38,286	0.2036	39,991	0.1016	37,791	0.2186
9	38,525	0.1997	41,961	0.1838	39,991	0.1016
10	38,751	0.1935	43,439	0.1987	41,961	0.1838
11	39,097	0.5828	28,433	0.0004	43,439	0.1987

Table 2
Summary of quantum chemical calculations. Transition energy, g (from AM1 optimization) and transition assignments (from INDO/S) for monomer, dimer, trimer forms and the dimeric form of the trimer. NBF=number of basis functions

Oligomer	NBF	$\|\|\vec{g}\|\|$	Assignment	
			$S_0 \rightarrow S_1$ (cm^{-1}) (nm)	$S_0 \rightarrow S_3$ (cm^{-1}) (nm)
Monomer	208	2.66	28,090 (352) vw	29,032 (310) s
Dimer	408	2.86	29,070 (344) s	32,362 (309) s
Trimer	608	4.64	28,736 (348) s	33,223 (301) s
$(Trimer)_2$	1216	4.82	29,763 (336) w	31,348 (319) s

dimer and trimer forms (Fig. 9) of the isolated molecules. The transition energies for the electronic absorption spectra were determined using the well known formula [1,3] $E = \varepsilon_i - \varepsilon_a + J_{ia} \pm K_{ia}$ [15,16]. We have also calculated the oscillator strengths for each transition. Data are summarized in Table 1. Usually, configuration interaction (CI) calculations for conjugated polymer systems present CI vectors with large mixing. In particular, for this copolymer the calculated absorption spectra show an increasing resolution with the size of the polymer segment. For example, the spectrum of the monomer (Table 1) shows the expected large CI mixing, although it is still possible to obtain an approximate one electron picture for the spectrum. Among the three segments, the one composed by two mers (dimer) presents the calculated INDO/S spectrum with the closest resemblance to the experimental UV–visible spectrum obtained in chloroform (Fig. 5). This calculated spectrum is composed by two transitions at the same region: one low lying at 29,070 cm^{-1} and one higher energy at 23,620 cm^{-1} (Table 2). Finally, it is easy to trace the character of each transition down to a single excitation which in the case of the trimer can be assigned to the $S_0 \rightarrow S_1$ π,π^* transition. In all spectra we obtained a quite simple description in terms of an electron 'jump' between neighboring rings. Most transitions consist of excitations from an occupied π orbital 'localized' in a 2,5-dimethoxy-phenoxy moiety to an unoccupied π^* orbital of a phenyl ring in the next neighboring monomeric unit. The profile of the MOs involved in each transition suggests that all excitations tend to transfer the electron from the middle towards the end of the segment.

As an attempt to represent the absorption spectrum of aggregates we simulate the spectrum of a π stack of two segments of the trimer, whose geometry has also been optimized (Fig. 10). The calculated interplanar distance of species is ca. 4.7 Å. Interestingly enough, this distance was maintained during a full geometry optimization (not even symmetry constraints were imposed), suggesting that this association is remarkably stable. This distance is also in agreement with the experimental data from the Davidov splitting (3–5 Å).

4. Conclusions

The excitonic splitting found in the emission of the copolymer in concentrated conditions (concentrated solutions and solid state) was assigned to the fluorescence of associated forms, ca. ground state dimers or excimers, based on previous results obtained with substituted stilbenes. The presence of the former was confirmed by excitation spectra and results from an intermolecular association, since it they were seen only in concentrated conditions.

The PL of the copolymer films is redshifted in relation to the concentrated solution spectrum with $\varpi_{em} = 22{,}222\ cm^{-1}$ (450 nm) and a shoulder at $\varpi_{em} = 21{,}053\ cm^{-1}$ (475 nm). The electroluminescence spectrum peaks at 21,053 cm^{-1}, indicating that the electroluminescence is originated from the aggregates, that absorbed directly the excitation or were excited through energy transfer from the excited state of the isolated absorber. Both the substantially higher measured quantum yield and the longer monoexponential lifetime of the copolymer compared to stilbene agree with the greater rigidity and planarity of the polymer-tied chromophore in comparison with the free stilbene lumophore. To our knowledge, the lifetime for stilbene containing polymers is reported for the first time. Increase in planarity and rigidity favors the aggregation processes.

Acknowledgements

T.D.Z.A. and R.F.C. thank FAPESP, CNPq, FAEP/Unicamp and MCT/PADCT/IMMMP for financial support and fellowships. L.A. and A.M.M thank LACTEC, CNPq and IMMP for financial support. FEK thanks AFOSR for their support.

References

[1] Akcelrud L. Prog Polym Sci 2003;28:875.
[2] Yang Z, Sokolik I, Karasz FE. Macromolecules 1993;26:1188.
[3] Yang Z, Hu B, Karasz FE. Macromolecules 1995;28:6151.
[4] Kim DY, Cho HN, Kim CY. Prog Polym Sci 2000;25:1089.
[5] Hu B, E F. Karasz. Chem Phys 1998;227:263.
[6] Yang Z, Hu B, Karasz FE. J Macromol Sci, Pure Appl Chem 1998; A35:233.
[7] Hu B, Yang Z, Karasz FE. J Appl Phys 1994;76:2419.
[8] Sokolik I, Yang Z, Morton DC, Karasz FE. J Appl Phys 1993;74:3584.
[9] Hu B, Morton DC, Sokolik I, Yang Z, Karasz FE. J Lumin 1994; 60/61:919.
[10] Burn PL, Holmes AB, Kraft A, Brown AR, Bradley DDC, Friend RH. Mater Res Soc Symp Proc 1992;247:647.

[11] Zhang C, Braun D, Heeger AJ. J Appl Phys 1993;73:5177.
[12] Hsu JWP, Yan M, Jedju TM, Rothberg LJ, Hsieh BR. Phys Rev B 1994;49:712.
[13] Dewar MJS, Zoebisch EG, Healy EF, Stewart JJP. J Am Chem Soc 1985;107:3902.
[14] Dewar MJS, Zoebisch EG. J Mol Struct Theochem 1988;180.
[15] Ridley JE, Zerner MC. Theoret Chim Acta (Berlin) 1973;32:111.
[16] Zerner MC, Low GH, Kirchner RF, Mueller UT. Westerhoff. J Am Chem Soc 1980;102:589.
[17] Lackowicz JR. Principles of fluorescence spectroscopy. 2nd ed. New York: Kluwer Academic Publishers; 1999.
[18] Aguiar M, Pinto MR, Atvars TDZ, Akcelrud L, Saltiel J. J Photosci 2003;10:263.
[19] Kasha M, Rawls HR, El-Bayoumi MA. Pure Appl Chem 1965;11:371.
[20] Bortolato CA, Atvars TDZ, Dibbern-Brunelli D. J Photochem Photobiol A: Chem 1991;59:123.
[21] Birch DJ, Birks JB. Chem Phys Lett 1976;38:432.
[22] Taylor JR, Adams MC, Sibbett W. Appl Phys Lett 1979;35:590.
[23] Pyun C-H, Lyle TA, Daube GH, Park S-M. Chem Phys Lett 1986;124:48.
[24] Traylor JR, Adams MC, Sibbett W. J Photochem 1980;12:127.
[25] Charlton JL, Saltiel J. J Phys Chem 1977;20:1940.
[26] Woo HS, Lhost O, Graham SC, Brédas JL, Schenk R, Mullen K. Synth Met 1993;59:13.
[27] Tian B, Zerbi G, Schenk R, Mullen K. J Chem Phys 1991;95:3191.
[28] Ohnishi T, Doi S, Tsuchida Y, Noguchi T. IEEE Trans Electron Devices 1997;44:1253.
[29] Von Seggern H, Wnkel PS, Zhang C, Schimdt HW. Macromol J Chem Phys 1994;195:2023.
[30] Zheng S, Shi J, Mateu R. Chem Mater 2000;12:1814.
[31] Yang Z, Hu B, Karasz FE. J Macromol Sci, Pure Appl Chem 1998; A35:233.
[32] Burn PL, Holmes AB, Kraft A, Bradley DDC, Brown AR, Friend RH, Gymer RW. Nature 1992;356(6364):47.
[33] Zheng M, Ding L, Karasz FE. Macromol Chem Phys 2002;203:1337.
[34] Zheng M, Ding L, Lin Z, Karasz FE. Macromolecules 2002;35:9939.
[35] Chu Q, Pang Y, Ding L, Karasz FE. Macromolecules 2002;35:7569.
[36] Rothberg LJ, Yan M, Papadimitrakopoulos F, Galvin ME, Kwock FW, Miller TM. Synth. Met 1996;80:41.
[37] Cossiello RF, Akcelrud L, Atvars TDZ. J Braz Chem Soc. 2005;16:74.
[38] Conwell E. Phys Rev B 1997;57:218.
[39] Wu MW, Conwell E. Phys Rev B 1997;56:R10060.
[40] Samuel ID, Rumbles G, Collison CJ. Phys Rev B 1995;51:R11573.
[41] Kakubiak R, Rothberg LJ, Wan W, Hsieh BR. Synth Met 1999;101:230.
[42] Blatchford JW, Gustafson TL, Epstein AJ, Vandenbout D, Kerimo A, Higgins DA, et al. Phys Rev B 1996;54:R3683.
[43] Aguiar M, Figihara MC, Hummelgen IA, Peres LO, Garcia JR, Gruber J, et al. J Lumin 2002;96:219.
[44] Jenekhe AS, Á Osaheni J. Science 1994;265(5173):765.
[45] Aguiar M, Karasz FE, Akcelrud L. Macromolecules 1995;28:4598.
[46] Martin SJ, Cadby AJ, Lane PA, Bradley DDC. Synth Met 1999;101:665.